Nuclear Isomers in Nucleosynthesis

Brad Meyer
Clemson University

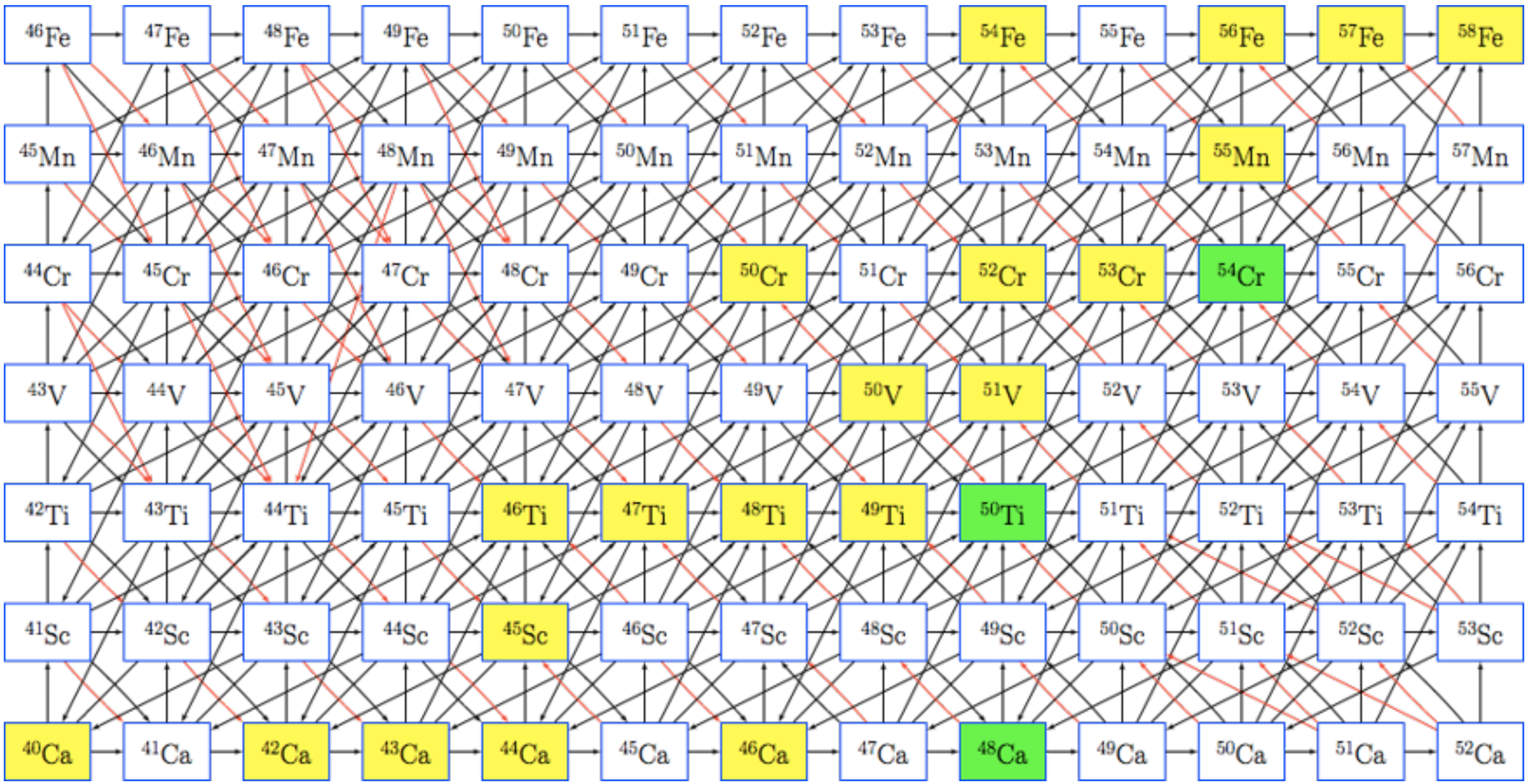
46Fe 47Fe 48Fe 49Fe 50Fe 51Fe 52Fe 53Fe 54Fe 55Fe 56Fe 57Fe 58Fe
45Mn 46Mn 47Mn 48Mn 49Mn 50Mn 51Mn 52Mn 53Mn 54Mn 55Mn 56Mn 57Mn
44Cr 45Cr 46Cr 47Cr 48Cr 49Cr 50Cr 51Cr 52Cr 53Cr 54Cr 55Cr 56Cr
43V 44V 45V 46V 47V 48V 49V 50V 51V 52V 53V 54V 55V
42Ti 43Ti 44Ti 45Ti 46Ti 47Ti 48Ti 49Ti 50Ti 51Ti 52Ti 53Ti 54Ti
41Sc 42Sc 43Sc 44Sc 45Sc 46Sc 47Sc 48Sc 49Sc 50Sc 51Sc 52Sc 53Sc
40Ca 41Ca 42Ca 43Ca 44Ca 45Ca 46Ca 47Ca 48Ca 49Ca 50Ca 51Ca 52Ca

Key assumption: all species internally equilibrated (=assumption that transitions between levels within a nuclear species occur more rapidly than reactions of the species with other species)

$$P_j \propto g_j \cdot e^{-E_j/kT}$$

This assumption not always true (especially for a species with a long-lived isomer)
=>must account for the transition rates among levels

“Astromers”

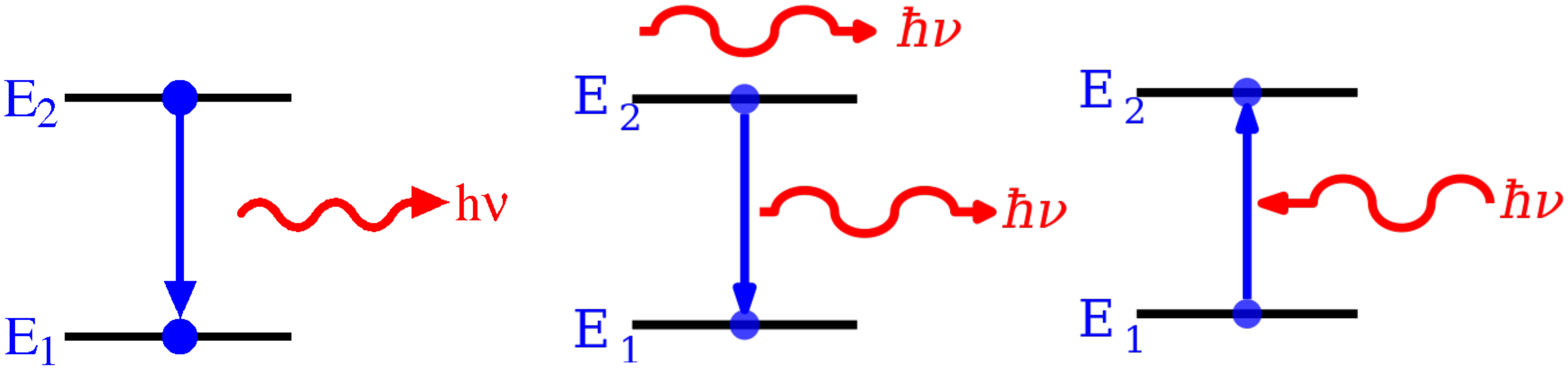

$A_{21} n_2$ $B_{21} n_2 \rho(\nu)$ $B_{12} n_1 \rho(\nu)$

$$\frac{B_{21}}{B_{12}} = \frac{g_1}{g_2}$$

$$\frac{A_{21}}{B_{21}} = \frac{2h\nu^3}{c^2}$$

^{26}Al

Gupta and Meyer (2001)

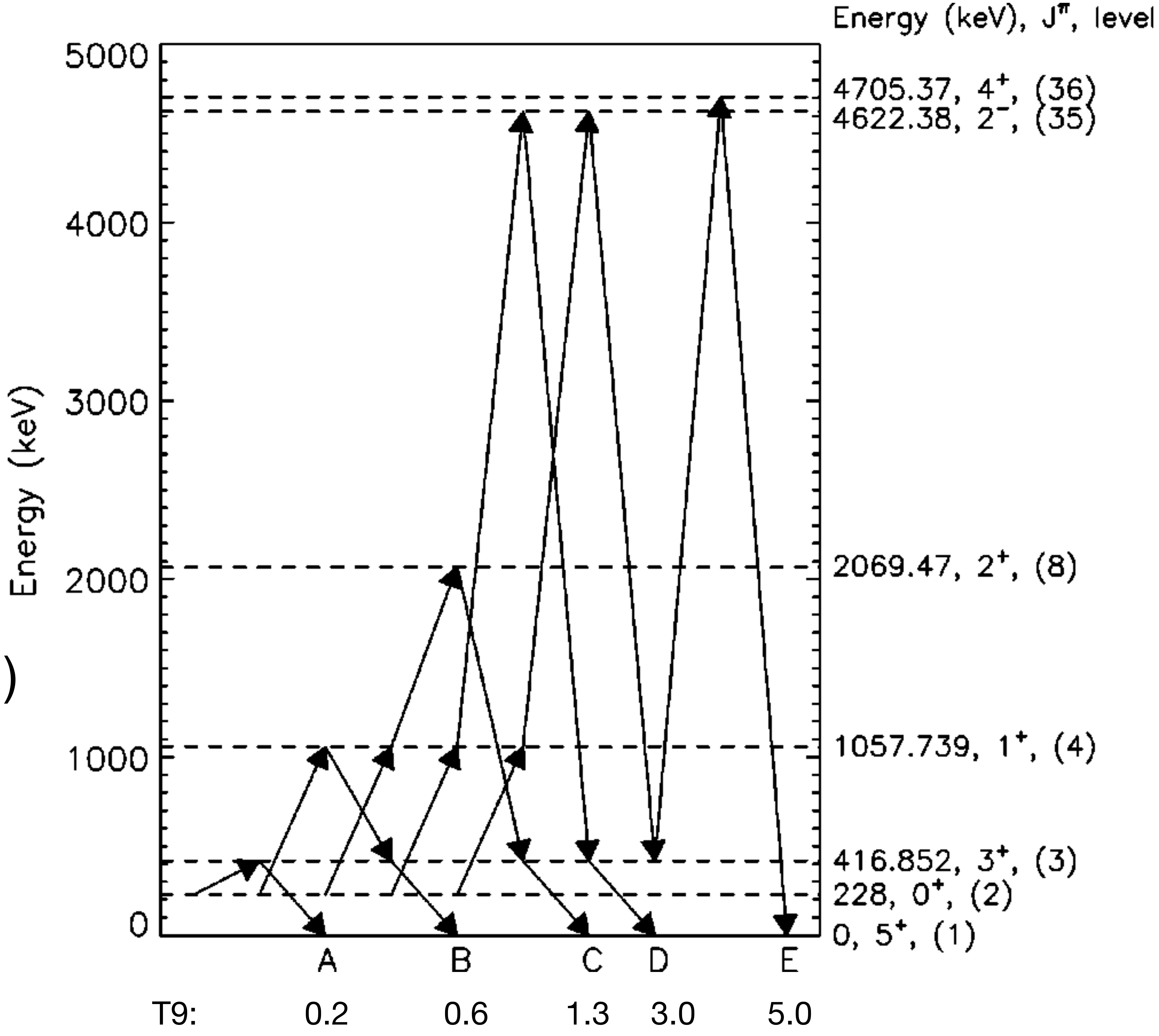

^{26}Al

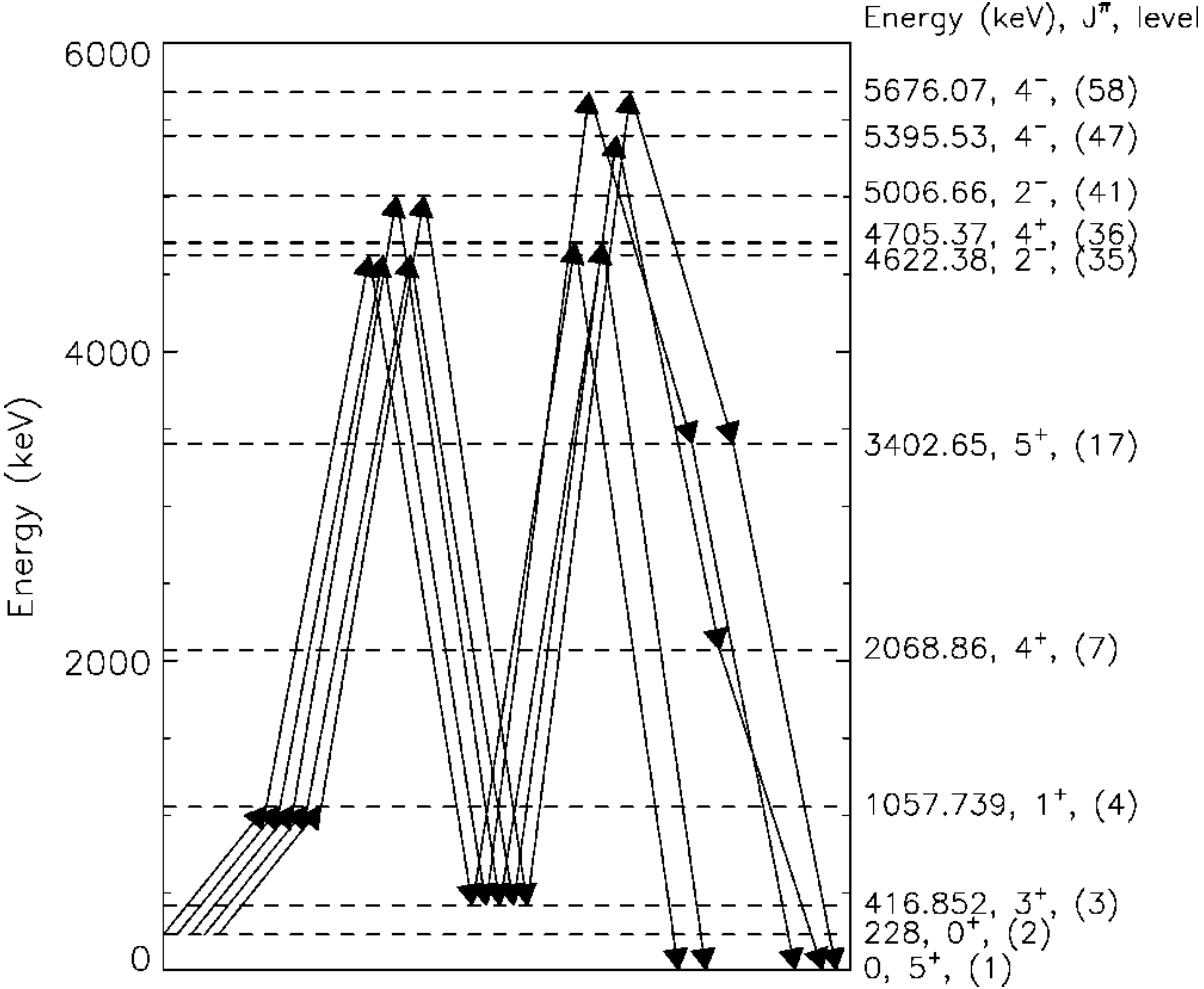

Energy (keV), J$^{\pi}$, level
6000
4000
2000
0
Energy (keV)
5676.07, 4$^-$, (58)
5395.53, 4$^-$, (47)
5006.66, 2$^-$, (41)
4705.37, 4$^+$, (36)
4622.38, 2$^-$, (35)
3402.65, 5$^+$, (17)
2068.86, 4$^+$, (7)
1057.739, 1$^+$, (4)
416.852, 3$^+$, (3)
228, 0$^+$, (2)
0, 5$^+$, (1)

^{26}Al

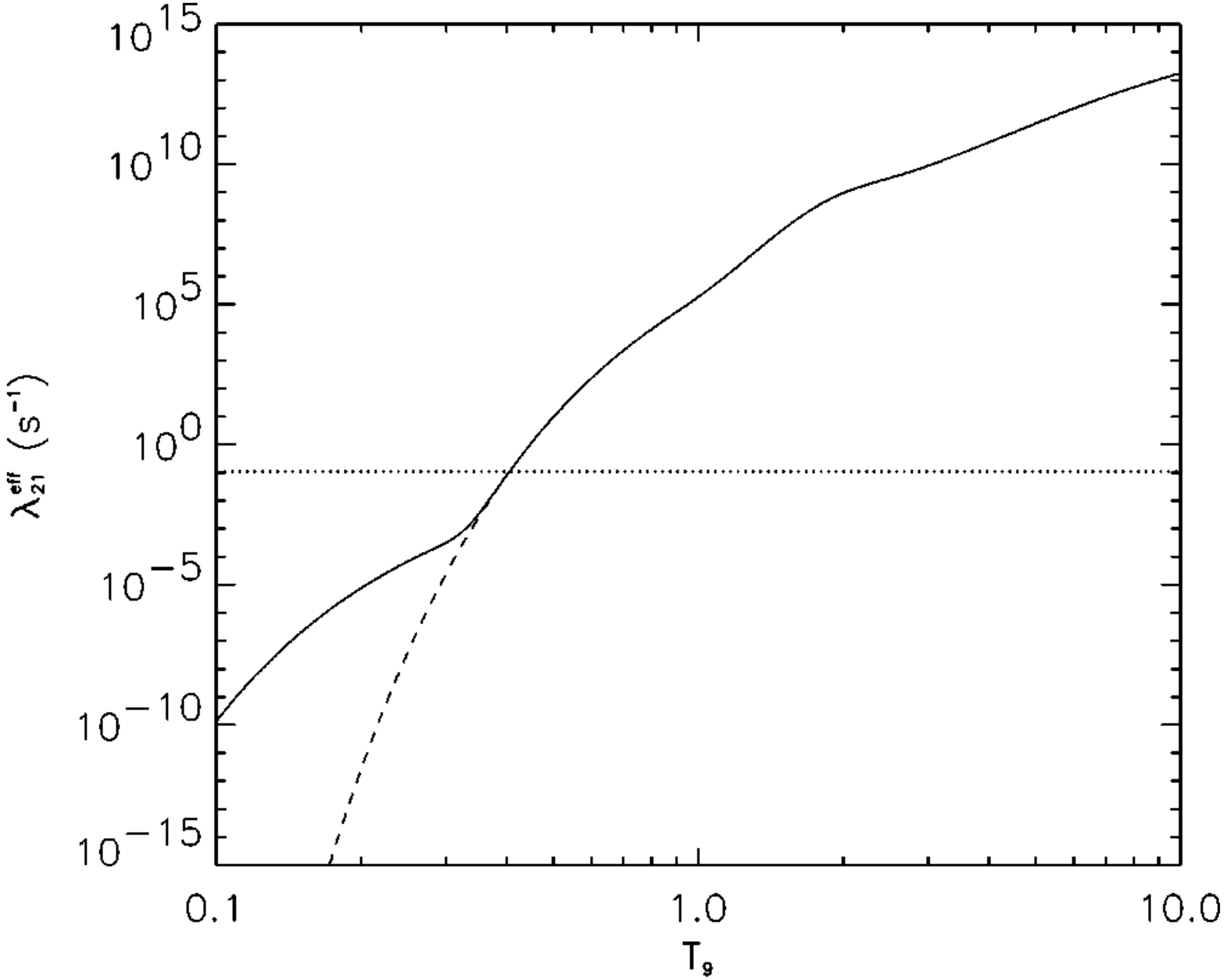

Effective isomerization rate

$$\lambda_{21}^{eff} = \sum_k \lambda_{2k}\Gamma_{k1}$$

$$\lambda_{21,3}^{eff} = \Lambda_2 \left\{ (f_{23} f_{24}) \begin{pmatrix} 1 + f_{34} f_{43} & f_{34} \\ f_{43} & 1 + f_{43} f_{34} \end{pmatrix} \begin{pmatrix} f_{31} \\ f_{41} \end{pmatrix} \right\}$$

$$= \Lambda_2 (\underbrace{\underbrace{f_{23} f_{31} + f_{24} f_{41}}_{\text{all two-arc paths}} + \underbrace{f_{23} f_{34} f_{41} + f_{24} f_{43} f_{31}}_{\text{all three-arc paths}} + \underbrace{f_{23} f_{34} f_{43} f_{31} + f_{24} f_{43} f_{34} f_{41}}_{\text{all four-arc paths}}}_{\text{effective branching ratio}}$$

Fugacity

$$\phi_k = X_k / X_k^{eq}$$

In upper-level steady state

$$\phi_k = \Gamma_{k1}\phi_1 + \Gamma_{k2}\phi_2$$

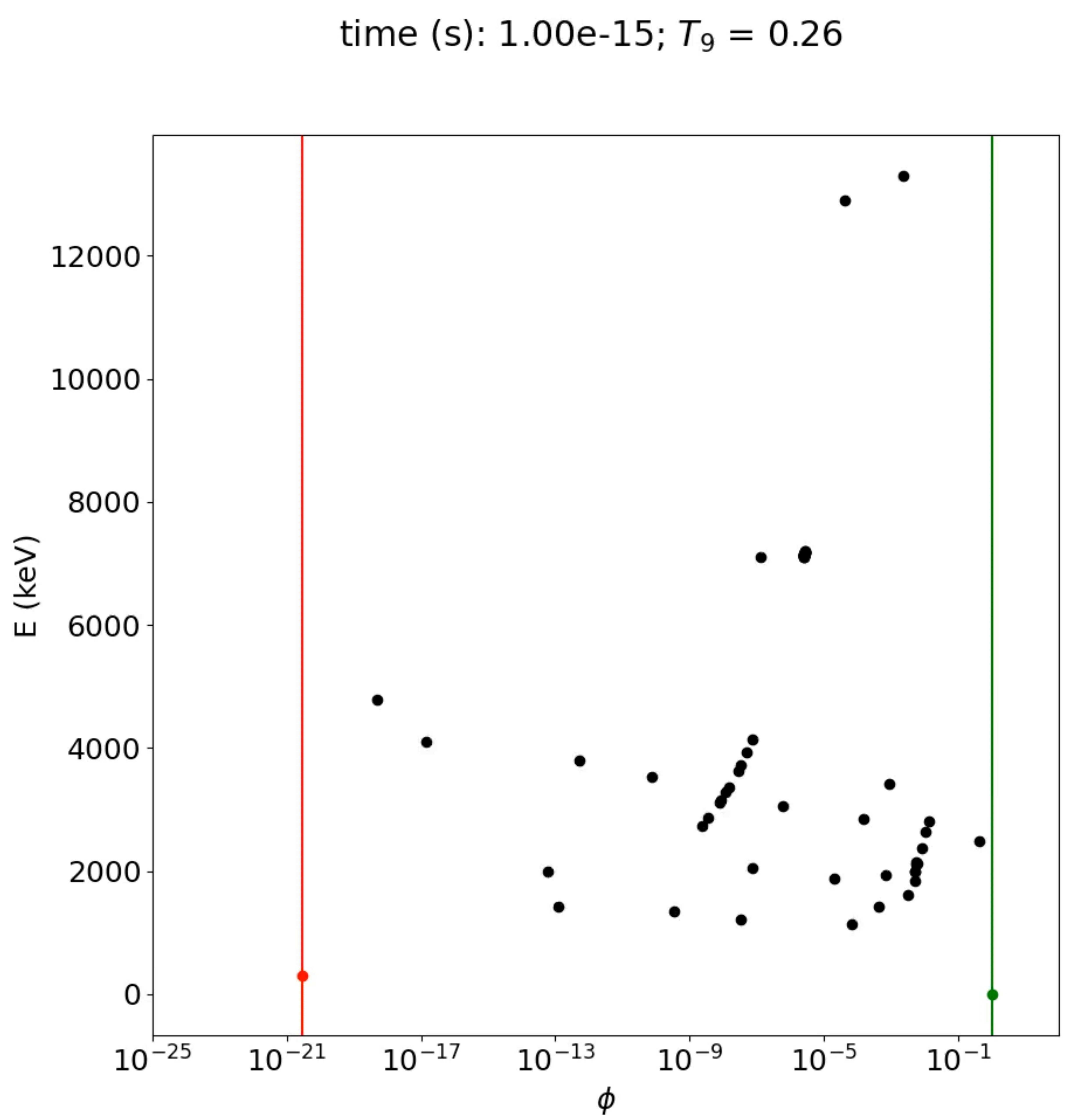

time (s): 1.00e-15; T_9 = 0.26
E (keV)
12000
10000
8000
6000
4000
2000
0
10^{-25}
10^{-21}
10^{-17}
10^{-13}
10^{-9}
10^{-5}
10^{-1}
ϕ

In upper-level steady state

$$\phi_k = \Gamma_{k1}\phi_1 + \Gamma_{k2}\phi_2$$

$$w_k^{(q)} = \begin{cases} \delta_{qk} & \text{if } k = 1,2, \\ \Gamma_{kq} R_{qk} & \text{if } k > 2 \ , \end{cases}$$

$$\lambda^{eff}_{(p,\gamma),q} = \left\{ \frac{(\lambda_{(p,\gamma)})^T w_q}{W_q} \right\}$$

^{87}Rb

- 27.8% of naturally occurring rubidium
- Produced in the s (slow) process of nucleosynthesis
- 49.2 Gyr lifetime (^{87}Rb—>^{87}Sr)
- During fractional crystallization, Sr tends to concentrate in plagioclase, so a residual magma may have an increased Rb/Sr ratio=>rock age can be determined from Rb and Sr concentrations and knowledge of the initial ^{87}Sr/^{86}Sr ratio

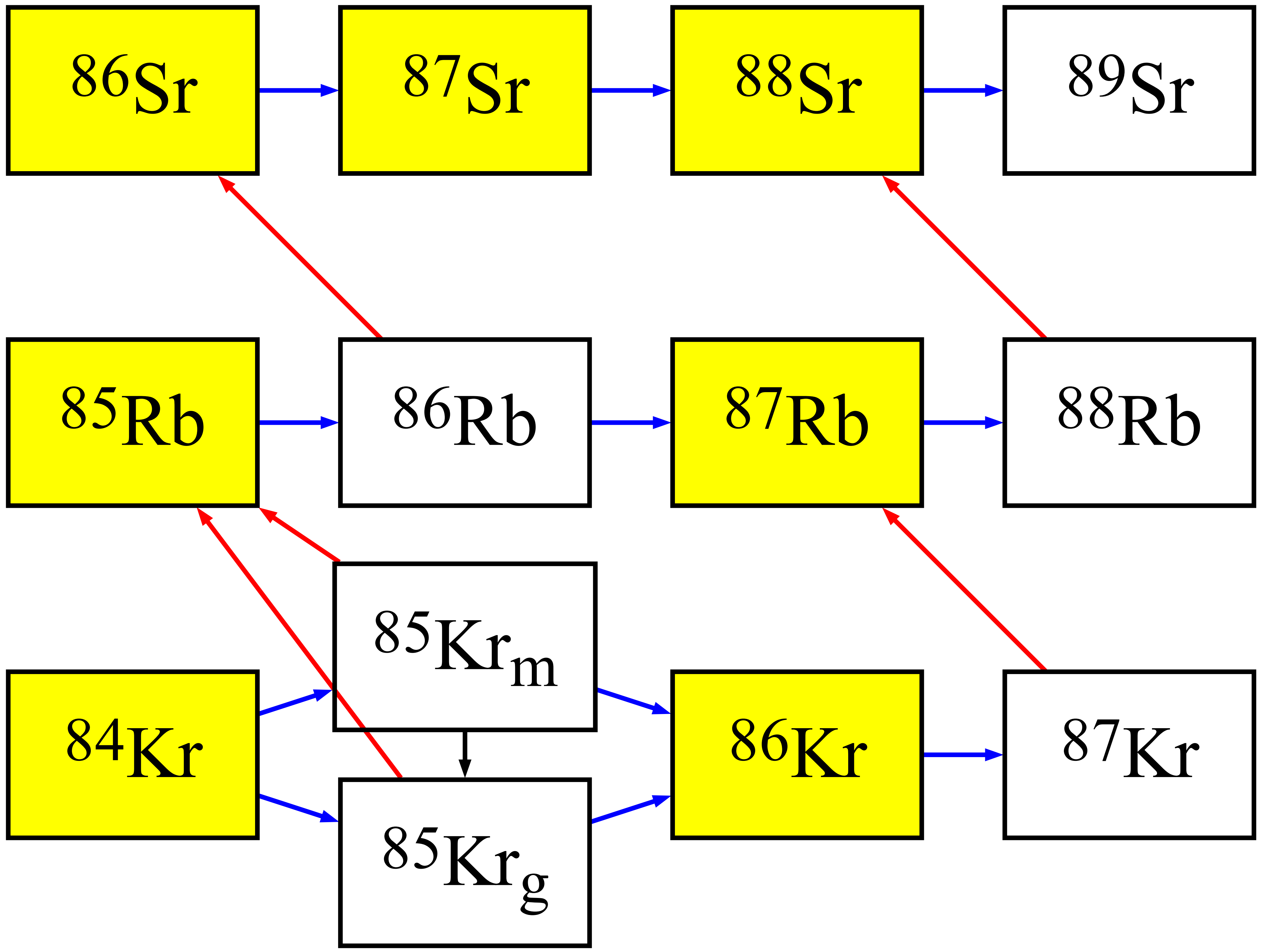

^{86}Sr
^{87}Sr
^{88}Sr
^{89}Sr
^{85}Rb
^{86}Rb
^{87}Rb
^{88}Rb
$^{85}Kr_m$
^{84}Kr
^{86}Kr
^{87}Kr
$^{85}Kr_g$

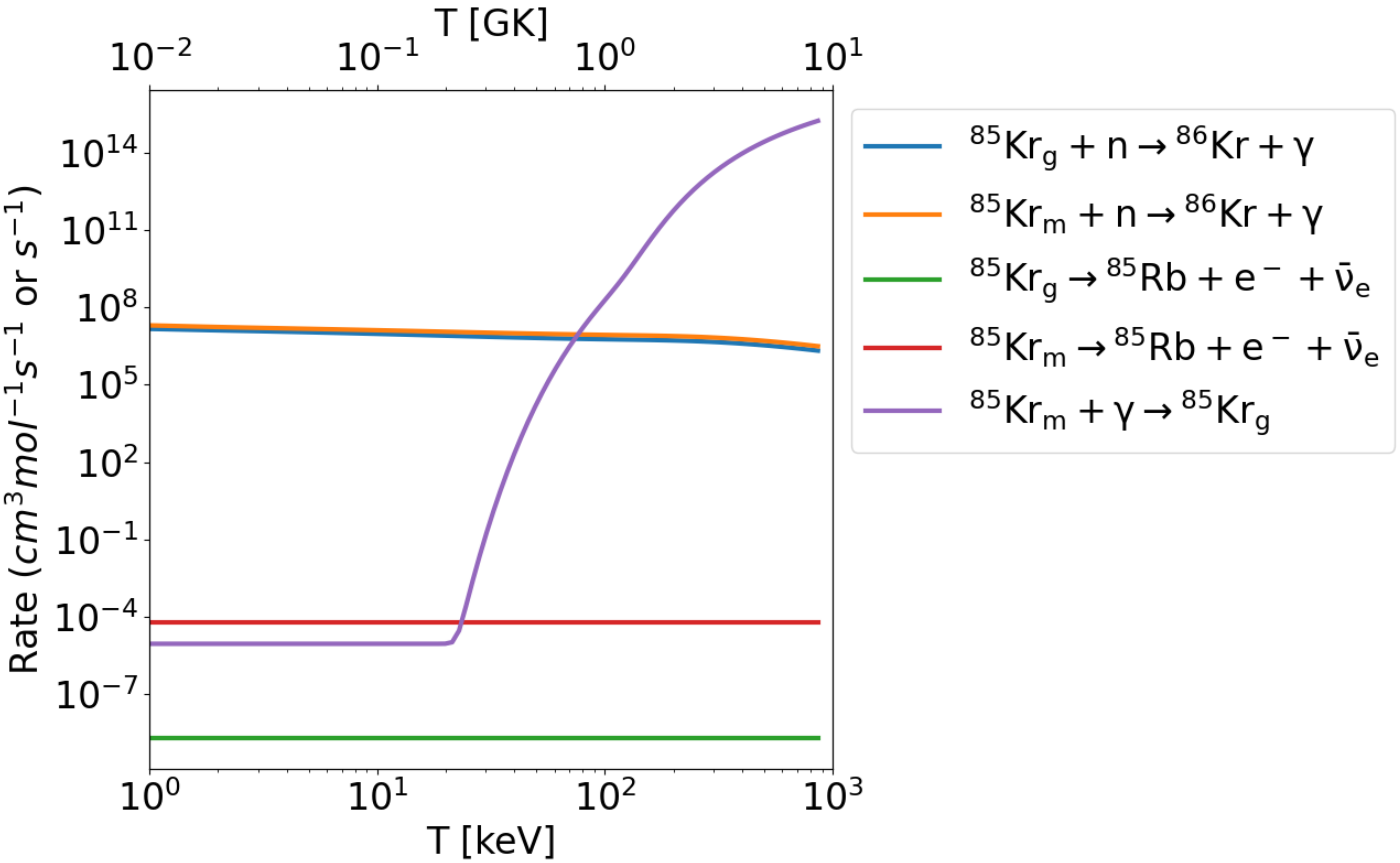

T [GK]
10^{-2}
10^{-1}
10^{0}
10^{1}
Rate ($cm^3 mol^{-1} s^{-1}$ or s^{-1})
10^{14}
10^{11}
10^{8}
10^{5}
10^{2}
10^{-1}
10^{-4}
10^{-7}
10^{0}
10^{1}
10^{2}
10^{3}
T [keV]
$^{85}Kr_g + n \rightarrow {}^{86}Kr + \gamma$
$^{85}Kr_m + n \rightarrow {}^{86}Kr + \gamma$
$^{85}Kr_g \rightarrow {}^{85}Rb + e^- + \bar{\nu}_e$
$^{85}Kr_m \rightarrow {}^{85}Rb + e^- + \bar{\nu}_e$
$^{85}Kr_m + \gamma \rightarrow {}^{85}Kr_g$

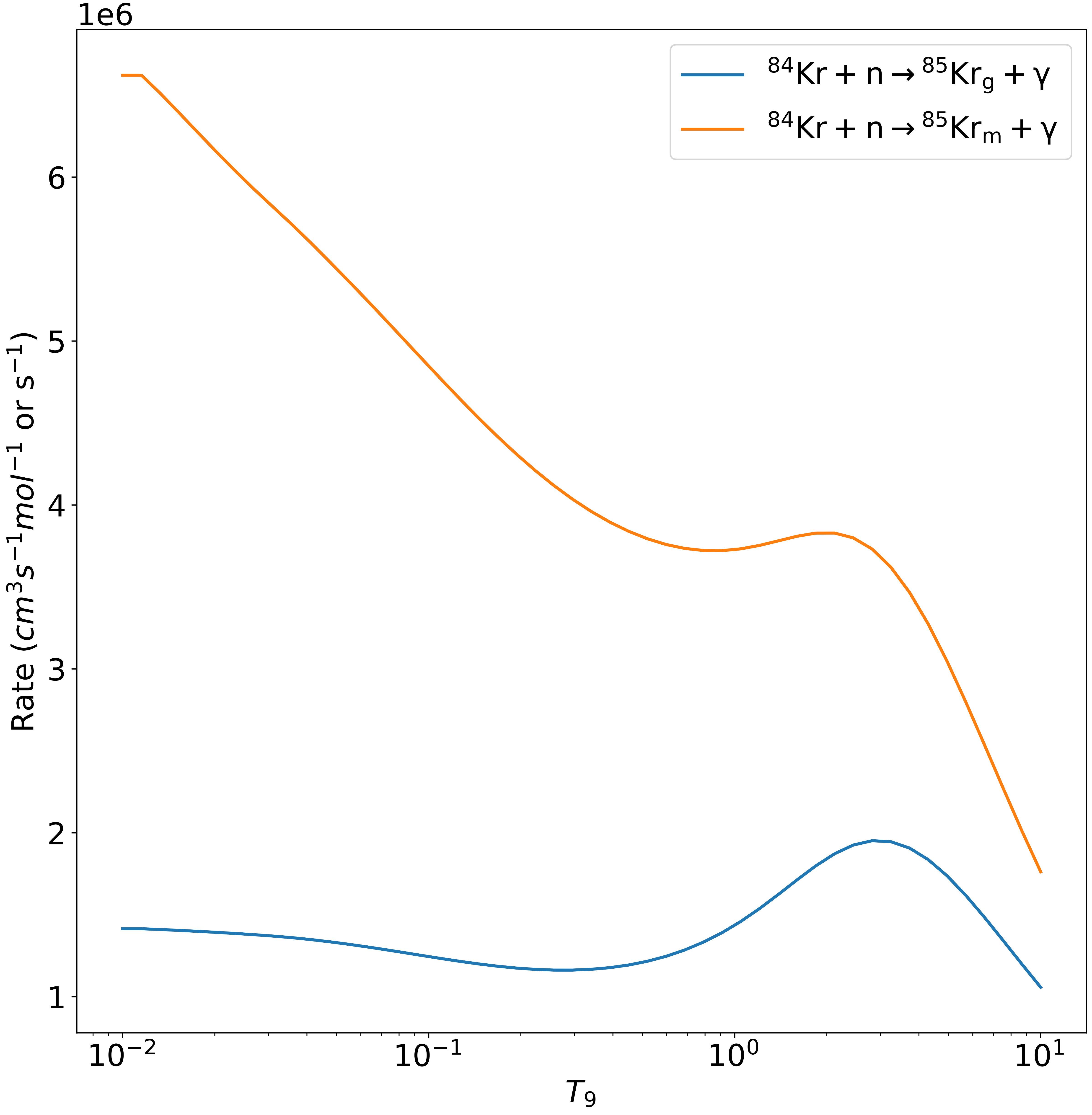

1e6
$^{84}Kr + n \rightarrow {}^{85}Kr_g + \gamma$
$^{84}Kr + n \rightarrow {}^{85}Kr_m + \gamma$
Rate ($cm^3 s^{-1} mol^{-1}$ or s^{-1})
T_9
1
2
3
4
5
6
10^{-2}
10^{-1}
10^{0}
10^{1}

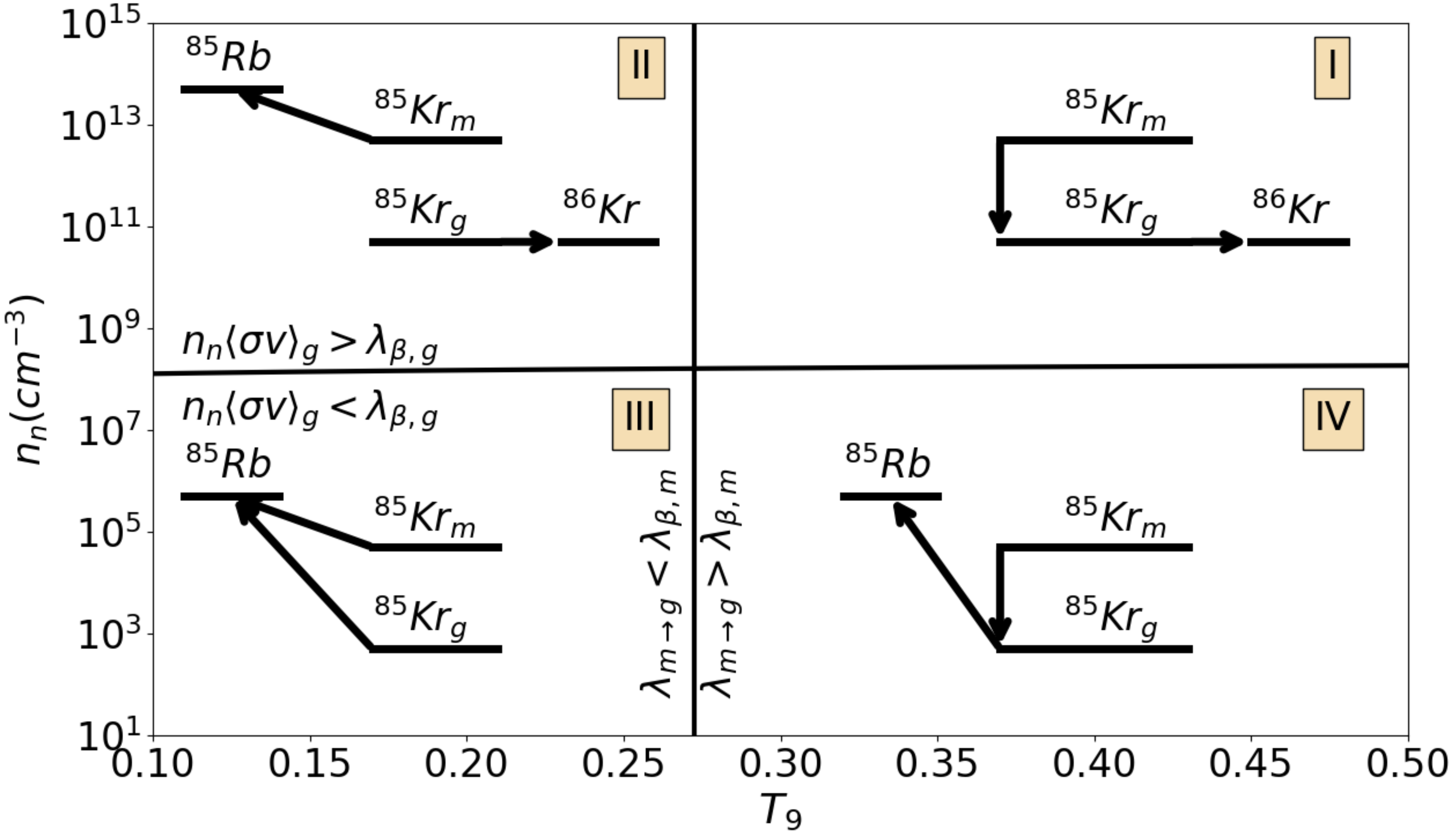

^{85}Rb
$^{85}Kr_m$
$^{85}Kr_g$
^{86}Kr
II
I
III
IV
$n_n\langle\sigma v\rangle_g > \lambda_{\beta,g}$
$n_n\langle\sigma v\rangle_g < \lambda_{\beta,g}$
$\lambda_{m\to g} < \lambda_{\beta,m}$
$\lambda_{m\to g} > \lambda_{\beta,m}$
$n_n(cm^{-3})$
T_9
10^{15}
10^{13}
10^{11}
10^{9}
10^{7}
10^{5}
10^{3}
10^{1}
0.10
0.15
0.20
0.25
0.30
0.35
0.40
0.45
0.50

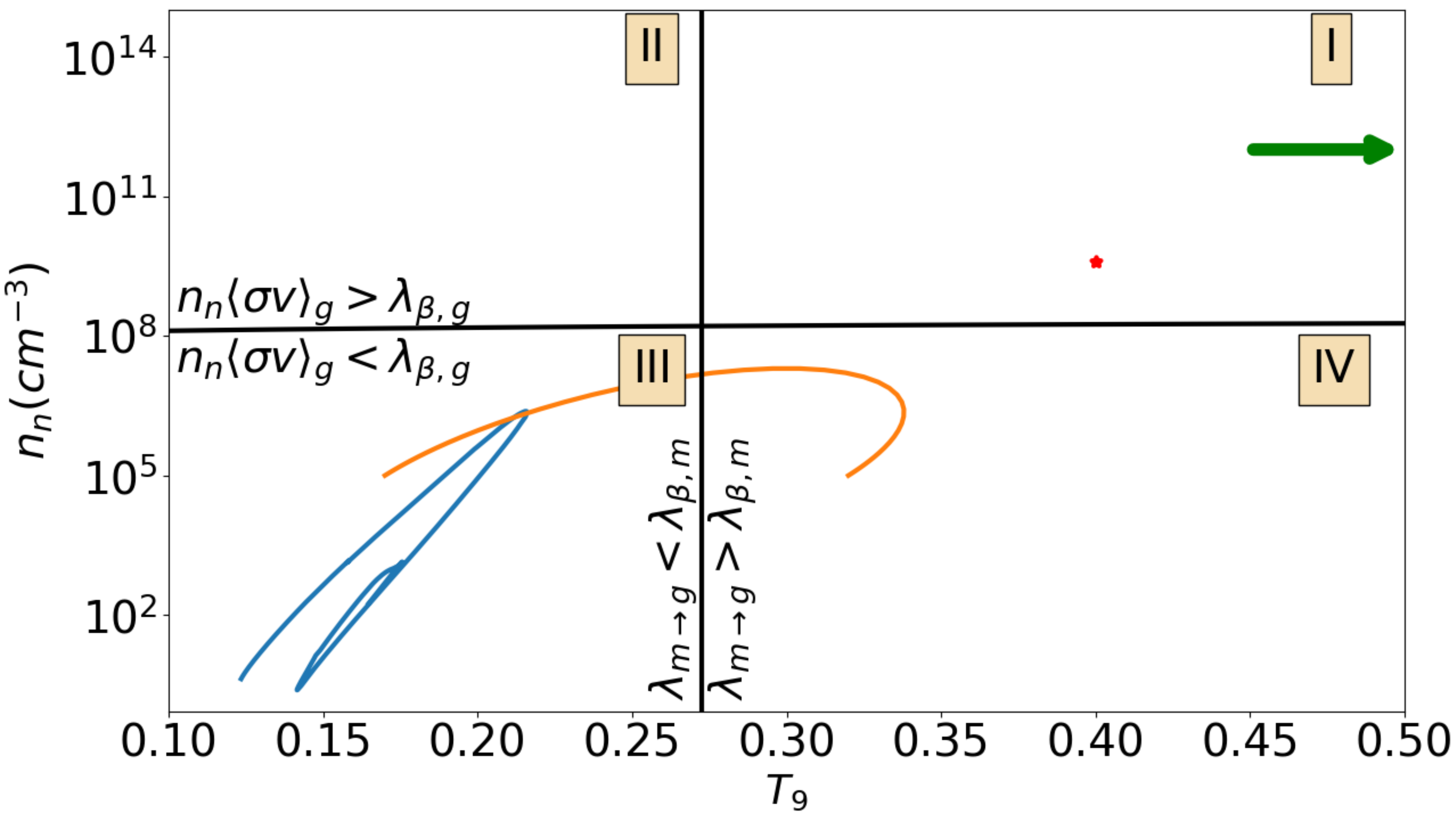

II
I
III
IV
$n_n\langle\sigma v\rangle_g > \lambda_{\beta,g}$
$n_n\langle\sigma v\rangle_g < \lambda_{\beta,g}$
$\lambda_{m\to g} < \lambda_{\beta,m}$
$\lambda_{m\to g} > \lambda_{\beta,m}$
10^{14}
10^{11}
10^{8}
10^{5}
10^{2}
$n_n(cm^{-3})$
0.10
0.15
0.20
0.25
0.30
0.35
0.40
0.45
0.50
T_9

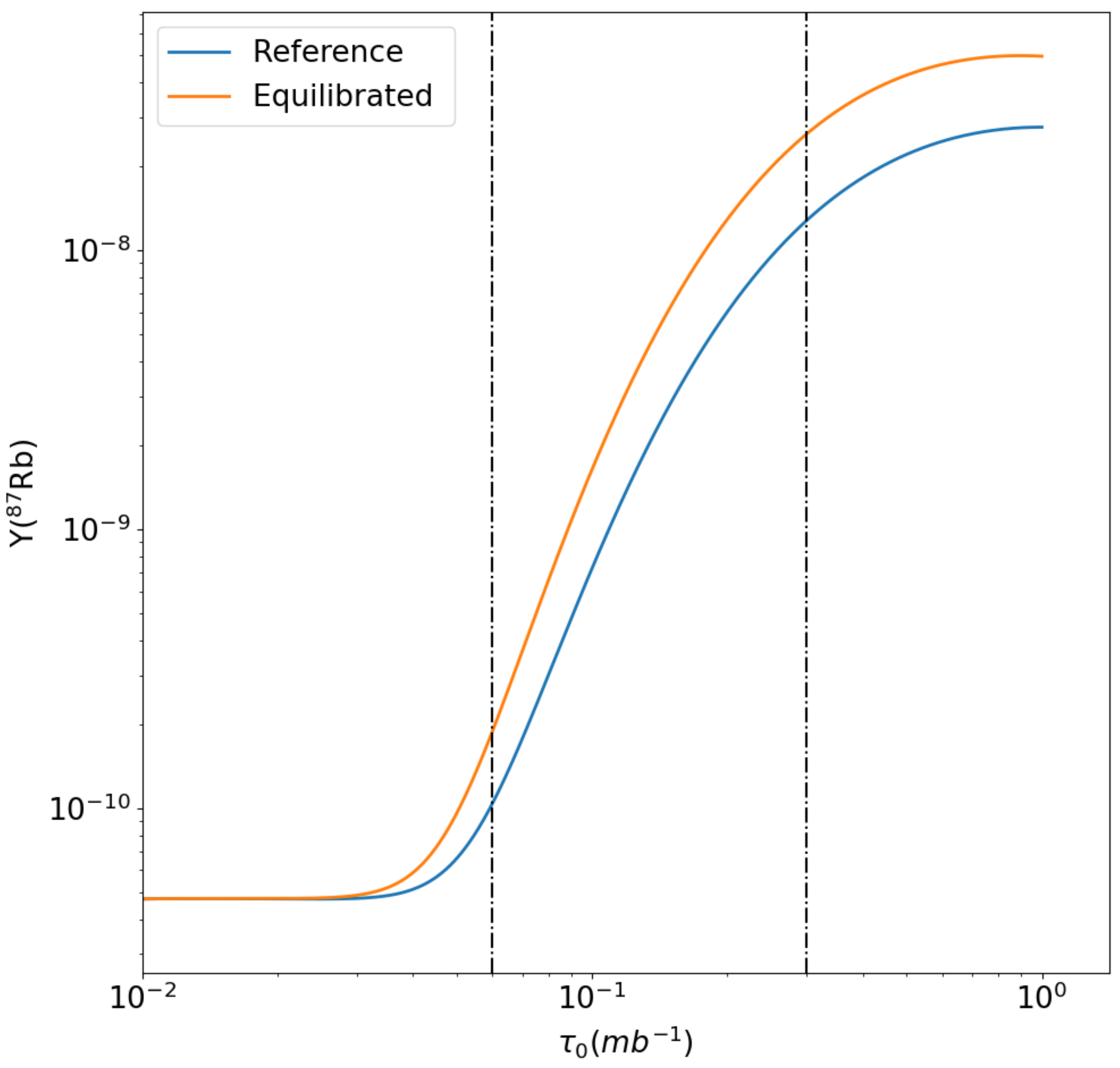

Massive Star

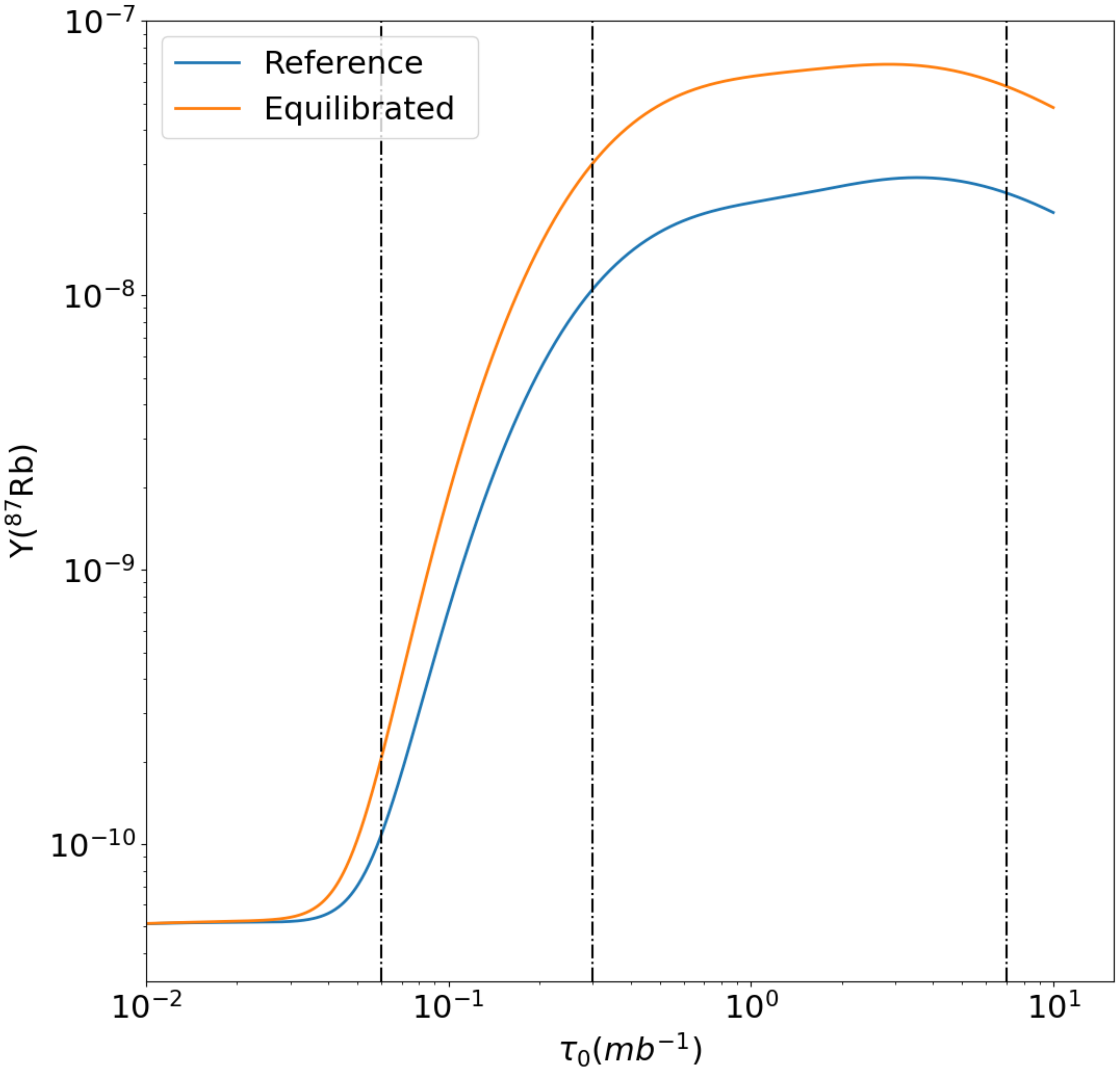

Reference
Equilibrated
10^{-7}
10^{-8}
10^{-9}
10^{-10}
$Y(^{87}Rb)$
10^{-2}
10^{-1}
10^{0}
10^{1}
$\tau_0(mb^{-1})$

TP AGB Star

Outlook and Future Work

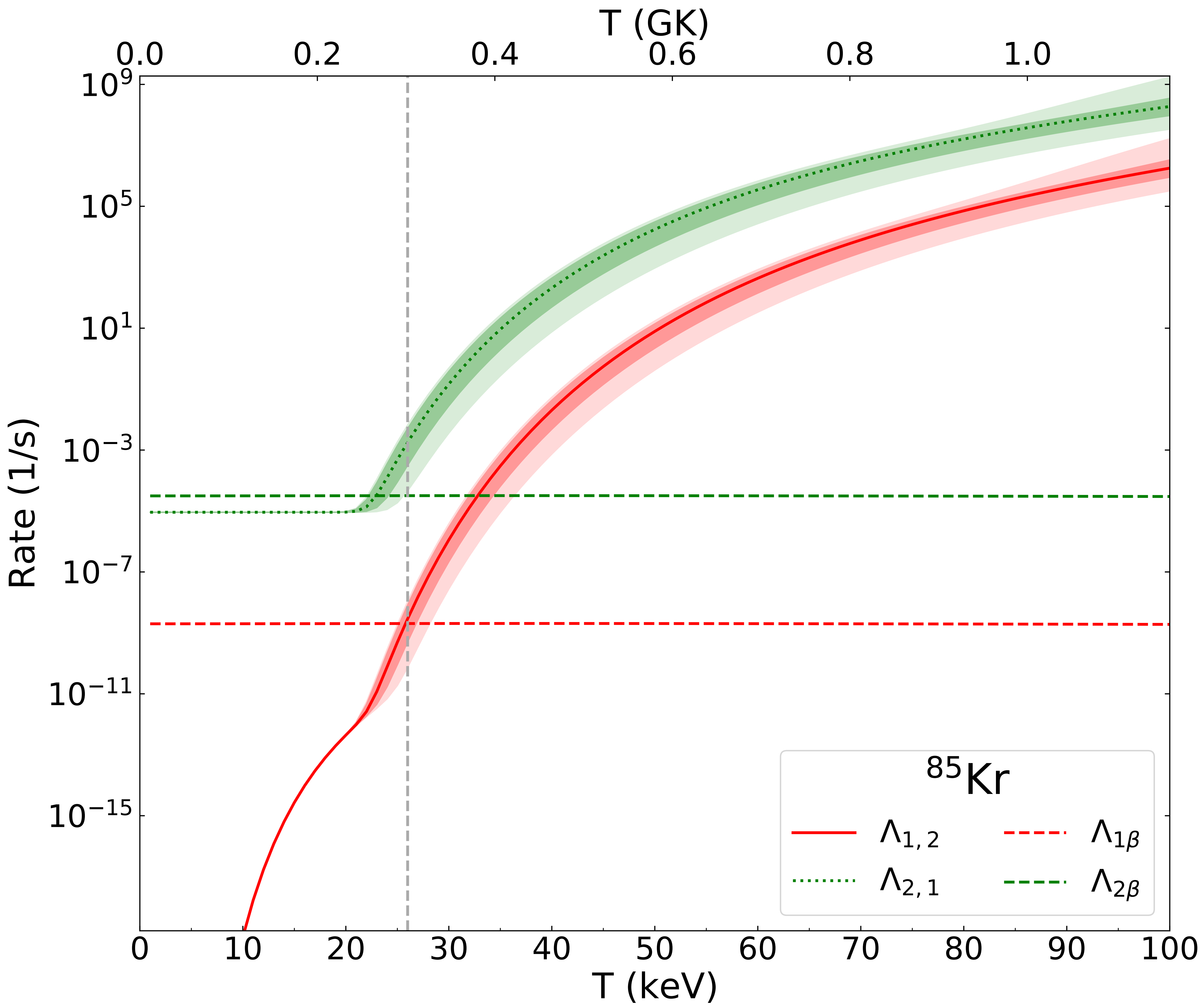

Misch et al. (2021)

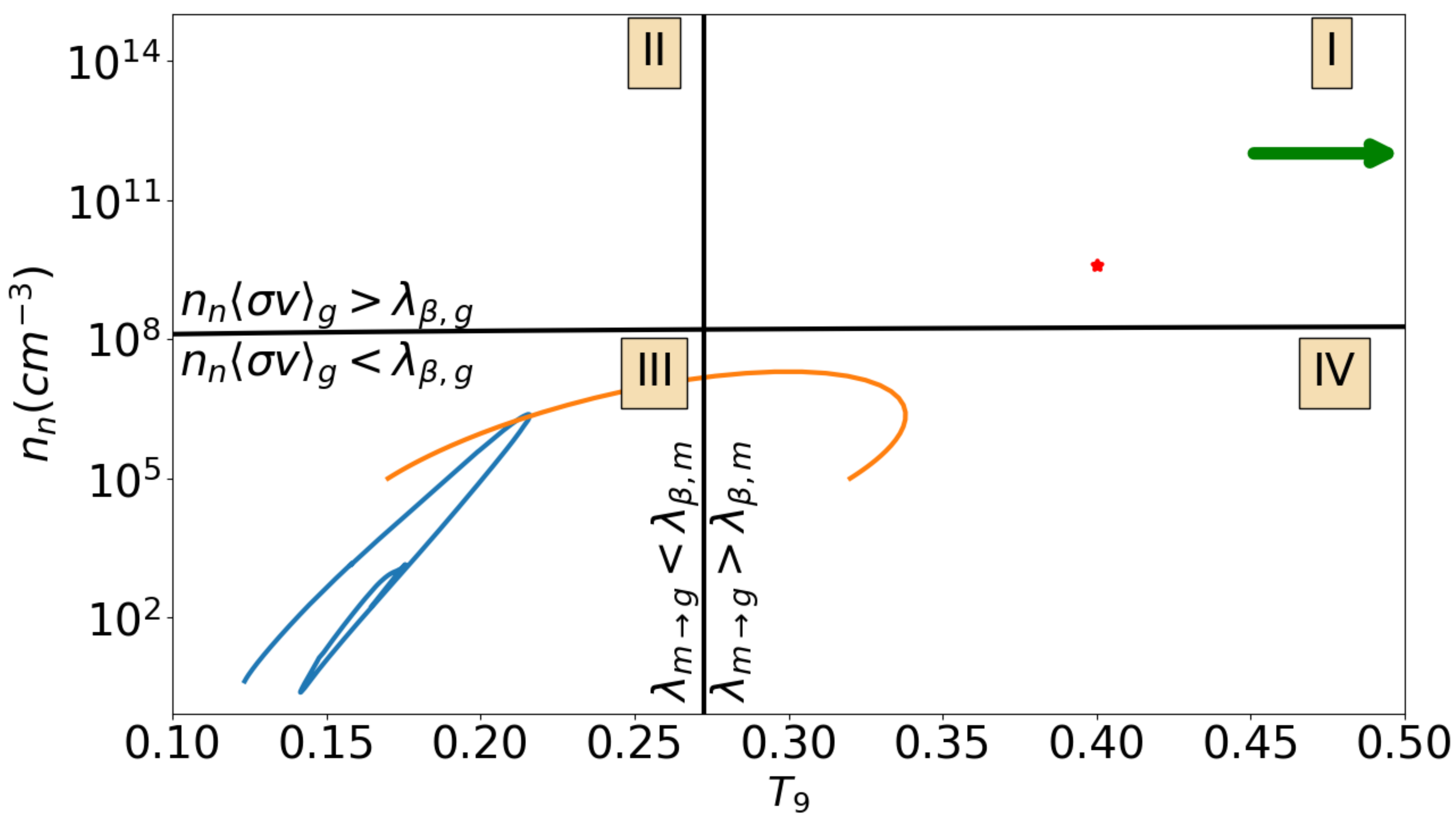

II
I
III
IV
$n_n\langle\sigma v\rangle_g > \lambda_{\beta,g}$
$n_n\langle\sigma v\rangle_g < \lambda_{\beta,g}$
$\lambda_{m\to g} < \lambda_{\beta,m}$
$\lambda_{m\to g} > \lambda_{\beta,m}$
10^{14}
10^{11}
10^{8}
10^{5}
10^{2}
$n_n(cm^{-3})$
0.10
0.15
0.20
0.25
0.30
0.35
0.40
0.45
0.50
T_9

Uncertainties dominated by unmeasured transition rates

1107.32 keV —> 304.871 keV

1140.73 keV —> 1107.32 keV

1166.69 keV —> 1140.73 keV

1166.69 keV —> 304.871 keV

1223.98 keV —> 1140.73 keV

1223.98 keV —> 1166.69 keV

1416.57 keV —> 1107.32 keV

Processes Affected

- S process
- I process
- R Process (especially decay back to stability)

Lvlspy

- Python package developed by Jaad Tannous and myself for handling general quantum level systems
- Computes necessary rates in an astrophysical plasma and the appropriate rate matrix
- Available from https://lvlspy.readthedocs.io or https://webnucleo.readthedocs.io

Formalism

- Graph-theory treatment (Sayani Ghosh)
- Compute generalized cascade parameters from ratios of branchings on directed graphs rather than sum over all paths.
- Conceptually clearer and potentially more convenient computationally.